J Eng Math (2009) 63:279–292
DOI 10.1007/s10665-008-9229-z

Asymptotic analysis of the viscous micro/nano pump at low Reynolds number

Miccal T. Matthews · James M. Hill

Received: 17 May 2007 / Accepted: 19 March 2008 / Published online: 5 April 2008

Abstract The steady viscous parabolic flow past an eccentrically placed rotating cylinder is studied in the asymptotic limit of small Reynolds number. It is assumed that the flow around the rotating cylinder undergoes boundary slip described by the Navier boundary condition. This involves a single parameter to account for the slip, referred to as the slip length ℓ, and replaces the standard no-slip boundary condition at solid boundaries. The streamlines for $\ell > 0$ are closer to the body than for $\ell = 0$, and it is discovered that the loss of symmetry due to the rotation of the cylinder is significantly reduced by the inclusion of slip. This arises as a result of a balance between the rotation velocity and the slip velocity on that portion of the cylinder which rotates opposite to the free-stream flow. Streamline patterns for nonzero eccentricity partially agree with Navier–Stokes simulations of the viscous pump; the small discrepancy is primarily due to the fact that here wall effects are not explicitly considered. Expressions for the frictional drag and the torque on the cylinder are obtained. The expression for the torque agrees well with the lubrication solution for the flow past a rotating cylinder placed symmetrically in a fully developed channel flow. The results presented here may be used to validate numerical schemes developed to study the viscous pump.

Keywords Asymptotic analysis · Navier boundary condition · Rotating cylinder · Viscous flow · Viscous pump

1 Introduction

The study of fluid mechanics at small scales is currently at the forefront of research in fluid mechanics due to the emergence of MEMS and NEMS (micro/nano-electro-mechanical systems) and LOC (lab-on-a-chip) technologies. The main hurdle to overcome in the design of micro/nanofluidic devices is the transport and pumping of small quantities of fluids. At small length scales a novel pump known as the viscous pump has been developed by Sen et al. [1], and it essentially consists of a transverse–axial cylindrical rotor eccentrically placed in a channel, so that the viscous resistance between the small and large gaps between the cylinder and the channel walls generate a net flow along the channel. Several numerical investigations appear in the literature, in particular those of Abdelgawad et al. [2] and Sharatchandra et al. [3,4]. The only analytical investigations to date apply the hydrodynamic theory of lubrication, as in [5] and more recently by Matthews and Hill [6].

M. T. Matthews (✉) · J. M. Hill
Nanomechanics Group, School of Mathematics and Applied Statistics, University of Wollongong, Wollongong, NSW 2522, Australia
e-mail: miccal@uow.edu.au

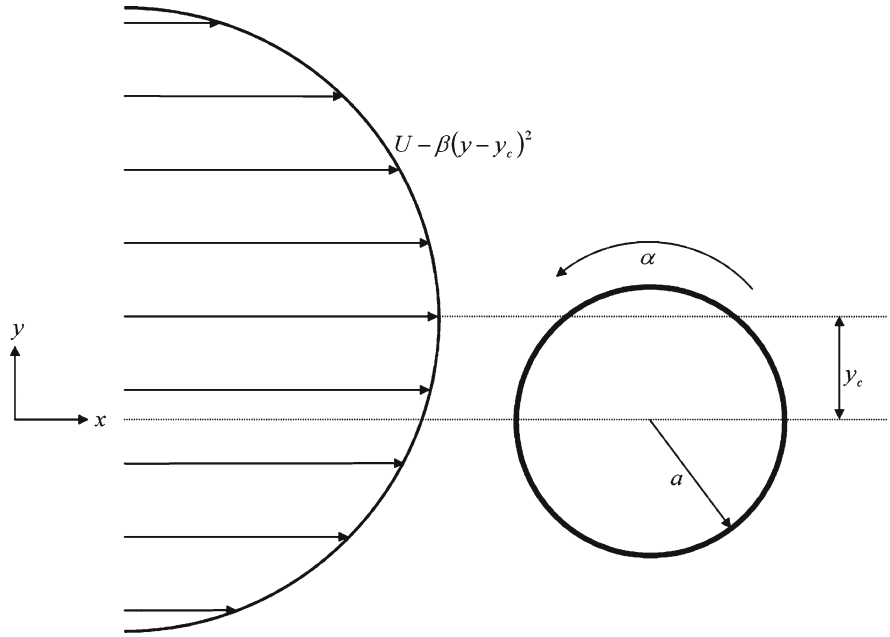

Fig. 1 Schematic diagram of problem geometry

Lubrication theory assumes that the distance of the rotating cylinder from the channel walls is much smaller than the diameter of the cylinder. To obtain a model applicable when the distance is much larger than that of the radius of the cylinder, we need to solve the Stokes flow equations, since fluid flow at the micro and nano scales is characterized by low Reynolds numbers. However, as is well known with Stokes flows involving cylinders, Stokes's paradox [7] prevents an acceptable solution being found. The way to overcome this difficulty is demonstrated by Proudman and Pearson [8] for a cylinder in a uniform flow using the method of singular perturbation theory [9]. Uniform flow past a cylinder with slip is studied in detail by Matthews and Hill [10], while shear flow past a rotating cylinder has been studied by Bretherton [11] and Robertson and Acrivos [12], and parabolic flow past a rotating sphere has been studied by Majhi and Vasudevaiah [13].

In the present analysis, we examine parabolic flow past a rotating cylinder placed eccentrically in the parabolic flow, in the limit of low Reynolds number using the method of matched asymptotic expansions. A schematic diagram of the problem geometry is shown in Fig.1. For simplicity, wall effects are not explicitly considered here, and the flow is assumed to correspond to fully developed parabolic flow. As detailed in the texts of Nguyen and Wereley [14] and Karniadakis et al. [15], there is experimental and molecular-dynamics evidence for the modification of the no-slip boundary condition for the study of small-scale devices such as the viscous micro/nanopump. Sharatchandra et al. [3] in their numerical work briefly study the effect of slip on the viscous pump, and they state that "further study of the mechanism of slip...is required" [3]. In this study it is assumed that there is slip on the surface of the rotating cylinder, with the degree of slip measured by a constant slip length as governed by the Navier boundary condition [16,17]. The results of this analysis may be used to validate numerical solutions of the viscous pump. In the next section, we formulate the mathematical problem describing parabolic flow past a eccentrically placed rotating cylinder. Next the asymptotic expansion procedure is described and the solution and forces acting on the cylinder are obtained. Finally, we present a discussion of the results and concluding remarks.

As a final comment, although the premise of the current work is to obtain analytical solutions for a rotating cylinder placed eccentrically in a parabolic flow, which may then be used to validate numerical studies for the viscous pump with a rotating cylinder which is off-set in a parabolic flow, the analysis presented here also has direct application to the field of particle dynamics. The motion of small objects suspended in a moving fluid is a fundamental problem in fluid mechanics and has been the subject of many detailed experimental, numerical and

analytical investigations. Happel and Brenner [18] give a thorough overview of Stokes-flow problems involving objects suspended in a viscous fluid, and the analysis presented here will expand on that knowledge.

2 Parabolic flow past an eccentrically placed rotating cylinder

Consider parabolic flow described by

$$v_x^*\left(y^*\right) = U^* - \beta\left(y^* - y_c^*\right)^2 \tag{2.1}$$

flowing past a micro/nano cylinder of radius a, which rotates about its axis with a constant angular velocity Ω. The center of the cylinder is placed eccentrically along the line $y_c^* = 0$. For dimensional consistency note that $U^*\,[=]\,L/T$ and $\beta\,[=]\,1/LT$. A cylindrical coordinate system (r^*, θ, z^*) will be used such that $x^* = r^*\cos\theta$, $y^* = r^*\sin\theta$ and

$$v_{r^*}^* = v_{x^*}^*\cos\theta + v_{y^*}^*\sin\theta,\ \ v_\theta^* = -v_{x^*}^*\sin\theta + v_{y^*}^*\cos\theta, \tag{2.2}$$

where $\Omega > 0$ in the direction of increasing θ. The boundary conditions at the cylinder surface are given by

$$r^* = a,:\ v_{r^*}^* = 0,\ v_\theta^* = a\Omega + \ell^*\left(\frac{\partial v_\theta^*}{\partial r^*} - \frac{v_\theta^*}{r^*}\right), \tag{2.3}$$

which are identical to those that are discussed in [10] with the inclusion of a rotation term. Away from the cylinder we have

$$r^* \to \infty\colon v_{x^*}^* = U^* - \beta\left(y^* - y_c^*\right)^2 \Rightarrow\ v_{r^*}^* = \left[U^* - \beta\left(r^*\sin\theta - y_c^*\right)^2\right]\cos\theta, \tag{2.4, 2.5}$$

$$v_\theta^* = -\left[U^* - \beta\left(r^*\sin\theta - y_c^*\right)^2\right]\sin\theta, \tag{2.6}$$

where ℓ^* is a constant slip length. It is assumed that

$$v_{r^*}^* = v_{r^*}\left(r^*, \theta\right),\quad v_\theta^* = v_\theta^*\left(r^*, \theta\right),\quad v_{z^*} = 0, \tag{2.7}$$

so that a stream function $\psi^*\left(r^*, \theta\right)$ defined by

$$v_{r^*}^* = \frac{1}{r^*}\frac{\partial\psi^*}{\partial\theta},\quad v_\theta^* = -\frac{\partial\psi^*}{\partial r^*}, \tag{2.8}$$

may be introduced such that the mass-conservation equation is automatically satisfied. In terms of this stream function the boundary conditions may be written

$$r^* = a\colon\ \frac{\partial\psi^*}{\partial\theta} = 0,\quad \ell^*\frac{\partial^2\psi^*}{\partial r^{*2}} - \left(\frac{\ell^*}{r^*} + 1\right)\frac{\partial\psi}{\partial r^*} - a\Omega = 0, \tag{2.9}$$

$$r^* \to \infty\colon\ \psi^* = U^* r^*\sin\theta - \frac{\beta}{3}\left(r^*\sin\theta - y_c^*\right)^3. \tag{2.10}$$

The Navier–Stokes equation in cylindrical coordinates with a stream function defined as above is given in [19]

$$\nu\nabla_{r^*}^4\psi^* = -\frac{1}{r^*}\frac{\partial\left(\psi^*, \nabla_{r^*}^2\psi^*\right)}{\partial\left(r^*, \theta\right)}, \tag{2.11}$$

where the Laplacian $\nabla_{r^*}^2$ is given by

$$\nabla_{r^*}^2 = \frac{\partial^2}{\partial r^{*2}} + \frac{1}{r^*}\frac{\partial}{\partial r^*} + \frac{1}{r^{*2}}\frac{\partial^2}{\partial\theta^2}. \tag{2.12}$$

By introducing the dimensionless variables $r = r^*/a$, $\mathbf{v} = \mathbf{v}^*/\beta a^2$, $U = U^*/\beta a^2$, $\psi = \psi^*/\beta a^3$, $\ell = \ell^*/a$, $\alpha = \Omega/\beta a$, $y_c = y_c^*/a$, the Navier–Stokes equation and boundary conditions become

$$\nabla_r^4 \psi = -\frac{R}{r} \frac{\partial \left(\psi, \nabla_r^2 \psi\right)}{\partial (r, \theta)}, \tag{2.13}$$

$$r = 1\colon \ \frac{\partial \psi}{\partial \theta} = 0, \quad \ell \frac{\partial^2 \psi}{\partial r^2} - (\ell + 1) \frac{\partial \psi}{\partial r} - \alpha = 0, \tag{2.14}$$

$$r \to \infty\colon \ \psi = Ur \sin\theta - \frac{1}{3} (r \sin\theta - y_c)^3, \tag{2.15}$$

where

$$\nabla_r^2 = \frac{\partial^2}{\partial r^2} + \frac{1}{r} \frac{\partial}{\partial r} + \frac{1}{r^2} \frac{\partial^2}{\partial \theta^2}, \tag{2.16}$$

and $R \equiv R^{(t)}$ is the dimensionless (translational) Reynolds number defined by $R = \beta a^3/\nu$. Note that $y_c = 0$ corresponds to the cylinder being centered on the channel axis.

3 Asymptotic analysis

The above set of equations are solved using the method of matched asymptotic expansions, where R is assumed to be the small parameter. Following the method of Proudman and Pearson [8], near the cylinder we have a Stokes expansion defined by

$$\psi (r, \theta; R) = \sum_{n=0}^{\infty} f_n (R) \psi_n (r, \theta), \tag{3.1}$$

where $1 \gg f_0 (R) \gg R$ and $f_{n+1} (R) / f_n (R) \to 0$ as $R \to 0$, and far from the cylinder we have an Oseen expansion defined by

$$\Psi (\rho, \theta; R) = \sum_{n=0}^{\infty} F_n (R) \Psi_0 (\rho, \theta), \tag{3.2}$$

where $F_{n+1} (R) / F_n (R) \to 0$ as $R \to 0$, $f_0 (R) = F_0 (R) = 1$, and Ψ and ρ are suitably defined Oseen variables such that the right-hand side of the Navier–Stokes equation is the same order as the left-hand side. To find the simplest such transformation for the Oseen variables we define $\rho = f (R) r$, $\Psi = g (R) \psi$. Substituting in the Navier–Stokes equation reveals that $g (R) = R$, while the requirement that the boundary condition at infinity is $O(1)$ implies $f (R) = R^{\frac{1}{3}}$. Thus, the Oseen variables are taken to be

$$\rho = R^{\frac{1}{3}} r, \quad \Psi = R\psi. \tag{3.3}$$

Hence, the Stokes expansion satisfies

$$\nabla_r^4 \psi = -\frac{R}{r} \frac{\partial \left(\psi, \nabla_r^2 \psi\right)}{\partial (r, \theta)}, \tag{3.4}$$

$$r = 1\colon \ \frac{\partial \psi}{\partial \theta} = 0, \quad \ell \frac{\partial^2 \psi}{\partial r^2} - (\ell + 1) \frac{\partial \psi}{\partial r} - \alpha = 0, \tag{3.5}$$

while the Oseen expansion satisfies

$$\nabla_\rho^4 \Psi = -\frac{1}{\rho} \frac{\partial \left(\Psi, \nabla_\rho^2 \Psi\right)}{\partial (\rho, \theta)}, \tag{3.6}$$

$$\rho \to \infty\colon \ \Psi = -\frac{1}{3} \rho^3 \sin^3\theta + R^{\frac{1}{3}} y_c \rho^2 \sin^2\theta + R^{\frac{2}{3}} \left(U - y_c^2\right) \rho \sin\theta, \tag{3.7}$$

where

$$\nabla_\rho^2 = \frac{\partial^2}{\partial \rho^2} + \frac{1}{\rho}\frac{\partial}{\partial \rho} + \frac{1}{\rho^2}\frac{\partial^2}{\partial \theta^2}. \tag{3.8}$$

The constant term $Ry_c^3/3$ in the boundary condition at infinity is neglected since the stream function is arbitrary to a constant.

3.1 Outer solution

Following the method of Majhi and Vasudevaiah [13], we first solve for the Oseen solution. The leading-order solution for the Oseen expansion which satisfies the following equation and boundary condition

$$\nabla_\rho^4 \Psi_0 = -\frac{1}{\rho}\frac{\partial\left(\Psi_0, \nabla_\rho^2 \Psi_0\right)}{\partial\left(\rho, \theta\right)}, \tag{3.9}$$

$$\rho \to \infty\colon\ \Psi_0 = -\frac{1}{3}\rho^3 \sin^3\theta, \tag{3.10}$$

is simply

$$\Psi_0\left(\rho, \theta\right) = -\frac{1}{3}\rho^3 \sin^3\theta, \tag{3.11}$$

as may be verified by direct substitution. By setting

$$F_1\left(R\right) = R^{\frac{1}{3}}, \tag{3.12}$$

the first-order solution for the Oseen expansion satisfies the following equation

$$\nabla_\rho^4 \Psi_1 = -\frac{1}{\rho}\left[\frac{\partial\left(\Psi_0, \nabla_\rho^2 \Psi_1\right)}{\partial\left(\rho, \theta\right)} + \frac{\partial\left(\Psi_1, \nabla_\rho^2 \Psi_0\right)}{\partial\left(\rho, \theta\right)}\right], \tag{3.13}$$

which must be solved subject to

$$\rho \to \infty\colon \Psi_1 = y_c \rho^2 \sin^2\theta, \tag{3.14}$$

and the solution is simply

$$\Psi_1\left(\rho, \theta\right) = y_c \rho^2 \sin^2\theta, \tag{3.15}$$

which again may be verified by direct substitution. By setting

$$F_2\left(R\right) = R^{\frac{2}{3}}, \tag{3.16}$$

the second-order solution for the Oseen expansion satisfies the following equation

$$\nabla_\rho^4 \Psi_2 = -\frac{1}{\rho}\left[\frac{\partial\left(\Psi_0, \nabla_\rho^2 \Psi_2\right)}{\partial\left(\rho, \theta\right)} + \frac{\partial\left(\Psi_2, \nabla_\rho^2 \Psi_0\right)}{\partial\left(\rho, \theta\right)} + \frac{\partial\left(\Psi_1, \nabla_\rho^2 \Psi_1\right)}{\partial\left(\rho, \theta\right)}\right], \tag{3.17}$$

which must be solved subject to

$$\rho \to \infty\colon\ \Psi_2 = \left(U - y_c^2\right)\rho \sin\theta, \tag{3.18}$$

and the solution is simply

$$\Psi_2\left(\rho, \theta\right) = \left(U - y_c^2\right)\rho \sin\theta, \tag{3.19}$$

which again may be verified by direct substitution.

If $F_3(R) = R$, the third-order solution for the Oseen expansion satisfies

$$\nabla_\rho^4 \Psi_3 = -\frac{1}{\rho}\left[\frac{\partial\left(\Psi_0, \nabla_\rho^2 \Psi_3\right)}{\partial(\rho,\theta)} + \frac{\partial\left(\Psi_3, \nabla_\rho^2 \Psi_0\right)}{\partial(\rho,\theta)} + \frac{\partial\left(\Psi_1, \nabla_\rho^2 \Psi_2\right)}{\partial(\rho,\theta)} + \frac{\partial\left(\Psi_2, \nabla_\rho^2 \Psi_1\right)}{\partial(\rho,\theta)}\right]. \tag{3.20}$$

This equation is an analogue of the Oseen equation for shear flow past a cylinder studied by Robertson and Acrivos [12], but slightly more complicated since this equation cannot be progressively solved for $\nabla_\rho^2 \Psi_3$ first. The shear-flow solution obtained by Robertson [20] involved a tedious amount of algebra, and the parabolic flow problem is more difficult, hence we do not attempt to obtain the corresponding higher-order terms for the Oseen expansion.

Thus the Oseen expansion has been determined as

$$\Psi(\rho,\theta) = -\frac{1}{3}\rho^3 \sin^3\theta + R^{\frac{1}{3}} y_c \rho^2 \sin^2\theta + R^{\frac{2}{3}}(U - y_c^2)\rho \sin\theta. \tag{3.21}$$

3.2 Inner solution

The leading-order solution for the Stokes expansion satisfies the biharmonic equation $\nabla_r^4 \psi_0 = 0$, which must be solved subject to

$$r = 1: \ \frac{\partial \psi_0}{\partial \theta} = 0, \quad \ell \frac{\partial^2 \psi_0}{\partial r^2} - (\ell + 1)\frac{\partial \psi_0}{\partial r} - \alpha = 0. \tag{3.22}$$

Assuming a solution of the form $\psi_0(r,\theta) = g_1(r) + g_2(r)\sin\theta + g_3(r)\cos(2\theta) + g_4(r)\sin(3\theta)$, we find

$$g_1(r) = A_1 r^2 \log r + A_2 r^2 + A_3 \log r + A_4, \tag{3.23}$$

$$g_2(r) = B_1 r^3 + B_2 r \log r + B_3 r + \frac{B_4}{r}, \tag{3.24}$$

$$g_3(r) = C_1 r^4 + C_2 r^2 + \frac{C_3}{r^2} + C_4, \tag{3.25}$$

$$g_4(r) = D_1 r^5 + D_2 r^3 + \frac{D_3}{r} + \frac{D_4}{r^3}, \tag{3.26}$$

where throughout A_i, B_i, C_i, D_i, E_i $(i = 1, 2, 3, 4)$ denote arbitrary integration constants. The boundary condition are

$$r = 1: \ g_i = 0 \ (i = 2, 3, 4), \quad \ell \frac{d^2 g_i}{dr^2} - (\ell + 1)\frac{dg_i}{dr} - \delta_{i1}\alpha = 0 \quad (i = 1, 2, 3, 4), \tag{3.27, 3.28}$$

where δ_{ij} is the Kronecker delta function. Invoking the 'principle of minimum singularity' (see [9]) we may set

$$A_1 = A_4 = B_2 = C_1 = D_1 = 0, \tag{3.29}$$

and applying the boundary conditions we find that

$$g_1(r) = A_2 r^2 - \frac{(\alpha + 2A_2)\log r}{1 + 2\ell}, \tag{3.30}$$

$$g_2(r) = B_1\left[r^3 - \frac{2r}{1 + 2\ell} + \frac{1 - 2\ell}{(1 + 2\ell)\, r}\right], \tag{3.31}$$

$$g_3(r) = C_2\left[r^2 + \frac{1}{(1 + 4\ell)\, r^2} - \frac{2(1 + 2\ell)}{1 + 4\ell}\right], \tag{3.32}$$

$$g_4(r) = D_2\left[r^3 - \frac{3(1 + 2\ell)}{(1 + 6\ell)\, r} + \frac{2}{(1 + 6\ell)\, r^3}\right]. \tag{3.33}$$

If we assume a priori that $f_1(R) \gg R$ for $R \ll 1$ then the first-order solution to the Stokes expansion satisfies the biharmonic equation $\nabla_{r^*}^4 \psi_1 = 0$, which must be solved subject to

$$r = 1: \ \frac{\partial \psi_1}{\partial \theta} = 0, \quad \ell \frac{\partial^2 \psi_1}{\partial r^2} - (\ell + 1)\frac{\partial \psi_1}{\partial r} = 0. \tag{3.34}$$

Assuming a solution of the form $\psi_1(r,\theta) = g_5(r)\sin\theta$, we find

$$g_5(r) = E_1 r^3 + E_2 r\log r + E_3 r + \frac{E_4}{r}, \tag{3.35}$$

which must be solved subject to

$$r = 1:\ g_5 = 0, \quad \ell\frac{d^2 g_5}{dr^2} - (\ell+1)\frac{dg_5}{dr} = 0. \tag{3.36}$$

Invoking the 'principle of minimum singularity' (see Van Dyke [9]) we may set $E_1 = 0$, and applying the boundary condition we find

$$g_5(r) = E_2\left[r\log r - \frac{r}{2(1+2\ell)} + \frac{1}{2(1+2\ell)r}\right]. \tag{3.37}$$

Hence the Stokes solution is found to be

$$\begin{aligned}\psi(r,\theta) = {} & A_2 r^2 - \frac{(\alpha+2A_2)\log r}{1+2\ell} + B_1\left[r^3 - \frac{2r}{1+2\ell} + \frac{1-2\ell}{(1+2\ell)r}\right]\sin\theta \\ & + C_2\left[r^2 + \frac{1}{(1+4\ell)r^2} - \frac{2(1+2\ell)}{1+4\ell}\right]\cos(2\theta) \\ & + D_2\left[r^3 - \frac{3(1+2\ell)}{(1+6\ell)r} + \frac{2}{(1+6\ell)r^3}\right]\sin(3\theta) \\ & + f_1(R)\,E_2\left[r\log r - \frac{r}{2(1+2\ell)} + \frac{1}{2(1+2\ell)r}\right]\sin\theta.\end{aligned} \tag{3.38}$$

Expanding the leading-order Stokes expansion in terms of the Oseen variable $\rho = R^{\frac{1}{3}} r$ yields

$$\begin{aligned}R\psi \sim {} & \left[B_1\sin\theta + D_2\sin(3\theta)\right]\rho^3 + R^{\frac{1}{3}}\left[A_2 + C_2\cos(2\theta)\right]\rho^2 \\ & + R^{\frac{2}{3}}\left[-\frac{2B_1}{1+2\ell} + f_1(R)\log\left(\frac{1}{R^{\frac{1}{3}}}\right)E_2\right]\rho\sin\theta.\end{aligned} \tag{3.39}$$

Using the result $\sin^3\theta = [3\sin\theta - \sin(3\theta)]/4$ and $\sin^2\theta = 1/2\,[1-\cos(2\theta)]$ and applying the asymptotic matching principle (see [9]), to match with Eq. 3.21 we must have

$$A_2 = \frac{y_c}{2}, \quad B_1 = -\frac{1}{4}, \quad C_2 = -\frac{y_c}{2}, \quad D_2 = \frac{1}{12}, \quad E_2 = U - \frac{1}{2(1+2\ell)} - y_c^2, \tag{3.40}$$

$$f_1(R) = \left[\log\left(\frac{1}{R^{\frac{1}{3}}}\right)\right]^{-1}, \tag{3.41}$$

and note that $f_1(R) \gg R$ for $R \ll 1$ as required. Hence, the Stokes expansion is

$$\begin{aligned}\psi(r,\theta) = {} & -\frac{\alpha\log r}{1+2\ell} + \frac{y_c}{2}\left(r^2 - \frac{2\log r}{1+2\ell}\right) \\ & - \frac{\left(r^2-1\right)\left[(1+2\ell)r^2 - 1 + 2\ell\right]\sin\theta}{4(1+2\ell)r} - \frac{y_c\left(r^2-1\right)\left[(1+4\ell)r^2 - 1\right]\cos(2\theta)}{2(1+4\ell)r^2} \\ & + \frac{\left(r^2-1\right)\left[(1+6\ell)r^2\left(r^2+1\right) - 2\right]\sin(3\theta)}{12(1+6\ell)r^3} + \frac{1}{4}\left[\log\left(\frac{1}{R^{\frac{1}{3}}}\right)\right]^{-1} \\ & \times\left(2U - \frac{1}{1+2\ell} - 2y_c^2\right)\left[2r\log r - \frac{r^2-1}{(1+2\ell)r}\right]\sin\theta,\end{aligned} \tag{3.42}$$

which matches completely with the outer solution.

4 Drag and torque

4.1 Frictional drag

The frictional drag is calculated from the force that the fluid exerts on the cylinder per unit length beyond the force attributable to the ambient and hydrostatic pressure. This force is calculated from the tangential and normal components of stress $\mathbf{T} = -p\mathbf{I} + 2\mu\mathbf{D}$ integrated around the surface of the cylinder. The x-component of the stress that the fluid exerts on the cylinder is $T_{rr}\cos\theta - T_{r\theta}\sin\theta$, so that the x-component of the force is

$$F_x = \int_0^{2\pi} \left(T_{rr}\cos\theta - T_{r\theta}\sin\theta\right)|_{r=a} a\,\mathrm{d}\theta, \tag{4.1}$$

where from [19] the two stress components are given by

$$T_{rr} = -p + 2\mu D_{rr} = -p + 2\mu\frac{\partial v_r}{\partial r}, \quad T_{r\theta} = 2\mu D_{r\theta} = \mu\left[r\frac{\partial}{\partial r}\left(\frac{v_\theta}{r}\right) + \frac{1}{r}\frac{\partial v_r}{\partial\theta}\right]. \tag{4.2}$$

The mean pressure near the cylinder is calculated from the Navier–Stokes equation consistent with the approximation employed for the Stokes expansion of the stream function. Recall that $\psi = \psi_0 + f_1(R)\,\psi_1$, where ψ_0 and ψ_1 both satisfy the biharmonic equation. The Navier–Stokes equations consistent with the approximation for ψ_0 and ψ_1, that is, neglecting the convective inertial term, are given in [19]:
r component:

$$\frac{\partial p}{\partial r} = \frac{\mu}{r^2}\left[r\frac{\partial}{\partial r}\left(r\frac{\partial v_r}{\partial r}\right) - v_r + \frac{\partial^2 v_r}{\partial\theta^2} - 2\frac{\partial v_\theta}{\partial\theta}\right], \tag{4.3}$$

θ component:

$$\frac{\partial p}{\partial\theta} = \frac{\mu}{r}\left[r\frac{\partial}{\partial r}\left(r\frac{\partial v_\theta}{\partial r}\right) - v_\theta + \frac{\partial^2 v_\theta}{\partial\theta^2} + 2\frac{\partial v_r}{\partial\theta}\right], \tag{4.4}$$

while the z-component yields $\partial p/\partial z = 0$. By calculating the r and θ components of velocity from the definition of the stream function, substituting into the Navier–Stokes equations and integrating yields an expression for p. We evaluate the pressure at $r = a$ and substitute this expression and the expressions for the r- and θ-components of velocity in the expression for F_x. Performing the required integration and referencing the force by the dynamic head $\rho U^2 a$ yields the following for the drag coefficient c_D

$$c_D = \frac{F_x}{\rho U^2 a} = \frac{4\pi f_1(R)}{R}\left[U - \frac{1}{2(1+2\ell)} - y_c^2\right] \tag{4.5}$$

$$= \frac{4\pi}{R}\left[\log\left(\frac{1}{R^{\frac{1}{3}}}\right)\right]^{-1}\left[U - \frac{1}{2(1+2\ell)} - y_c^2\right]. \tag{4.6}$$

This expression bears obvious similarities to the results for uniform flow past a non-rotating cylinder for no-slip by Kaplun [21] and slip by Matthews and Hill [10], but this analogy is misleading due to the nature of the expansion procedure and definition of the Reynolds number adopted here.

It is interesting to note that the drag coefficient can be zero, like that for parabolic flow past a sphere studied by Majhi and Vasudevaiah [13]. The expression reduces to zero for

$$U = \frac{1}{2(1+2\ell)} + y_c^2, \tag{4.7}$$

but also note that this implies $\psi_1 = 0$, and therefore allows a Stokes solution to this problem with $R = 0$. However, this may be viewed simply as an artifact of the analysis and the corresponding symmetry of the leading-order solution, with no physical relevance.

4.2 Torque

The torque L is calculated by integrating the tangential component of stress $T_{r\theta}$ around the surface of the cylinder via

$$L = \int_0^{2\pi} T_{r\theta}|_{r=a} a \mathrm{d}\theta, \tag{4.8}$$

which yields

$$L = -\frac{4\pi\,(\alpha + y_c)}{R\,(1 + 2\ell)}, \tag{4.9}$$

which obviously provides a relation between the torque and rotation rate. Mathematically then it appears that the torque can be zero, like that for shear flow past a sphere studied by Robertson and Acrivos [12], which has the implication that the cylinder can freely rotate. As will be explained in the discussion, the viscous pump requires α and y_c to have opposite signs.

5 Discussion and concluding remarks

In this study we have applied the method of matched asymptotic expansions to obtain an expression for the stream function describing the parabolic flow past an eccentrically placed rotating cylinder. This model contains five input parameters; namely the rotation rate α, offset position y_c, Reynolds number R, uniform velocity U and slip length ℓ. We have assumed that the rotation rate is positive in the direction of increasing θ in terms of the cylindrical coordinate system used, while the offset position is positive for a cylinder placed below the location of the maximum of the parabolic velocity profile, as shown in Fig. 1. For the viscous pump, however, when the cylinder is placed closer to the bottom plane and the flow is from left to right, the rotation rate is clockwise. In terms of the problem studied here, to compare results for the viscous pump α and y_c should have opposite signs, which implies that the torque can be zero.

Initially we study the case of varying U. Figure 2 illustrates streamline plots for $\alpha = -1$, $R = 0.1$, $y_c = 0$ and $\ell = 0$ for various values of U. When $U = 0$ the external flow field is actually moving from right to left, as demonstrated in Fig. 2a where the streamlines are dragged around to the upper portion of the cylinder since the rotation is clockwise. As U is increased the external flow field changes from right to left, to left to right, causing a change in the streamline pattern from being dragged around from the upper portion of the cylinder to the lower portion. As the value of U increases further the external flow field becomes uniform-like as the effects of the parabolic portion are decreased, as evident from the form of the external flow field $U - \beta y^2$. This is apparent from Fig. 2f, where close to the cylinder the streamlines are like those for the uniform flow past a rotating cylinder. This is also apparent from the expression for the stream function, Eq. 3.42, which for large U is identical to the leading-order solution for uniform flow past a cylinder found in [10], except for the numerical factor $3U$.

Next we study the case of varying y_c. Figures 2d and 3 illustrate streamline plots for $\alpha = -1$, $R = 0.1$, $U = 3$ and $\ell = 0$ for various values of y_c. When $y_c = 0$ we can see from Fig. 2d that above and below the cylinder there are regions where the streamlines reverse their direction. As y_c increases, the reversed streamlines below the cylinder move up until they are at either side of the cylinder, and as y_c increases further they disappear. The reversed streamlines above the cylinder move closer to each other, join and then reverse the other way, so that an eddy forms with a center directly above the cylinder. As y_c increases further, the streamlines compact around the body and the reversed streamlines and eddy disappear and generally become like that for uniform flow past a cylinder. This can be seen from the expression for the stream function, Eq. 3.42, which for large y_c the y_c^2 term dominates and hence becomes identical to the leading-order solution for uniform flow past a cylinder as found in [10] except for the numerical factor $-3y_c^2$. Also we note that Fig. 3a is for zero torque, since $\alpha = -1$ and $y_c = 1$.

Before we continue with a discussion concerning the effects of slip, comparisons with previous work with no-slip will be made. We compare our results to that of Day and Stone [5] and Matthews and Hill [6] who both employ a

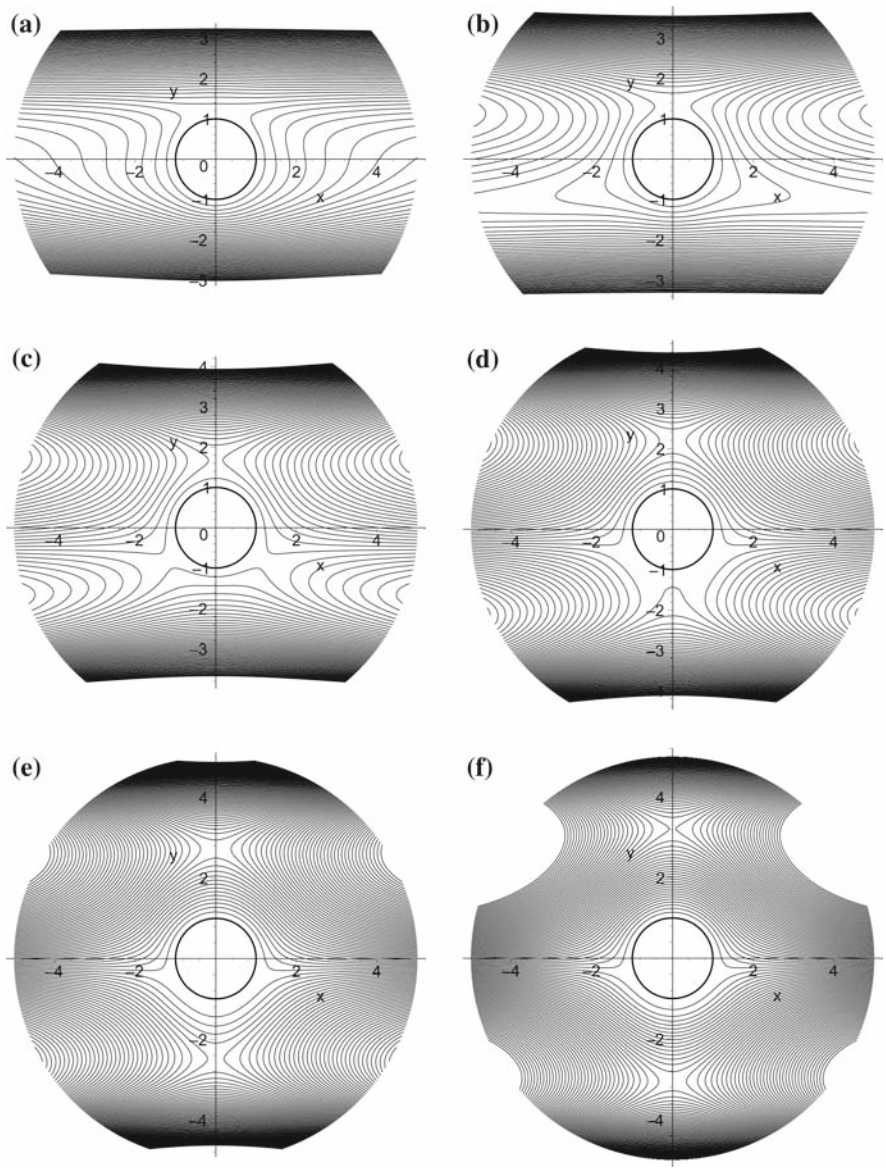

Fig. 2 Streamline plots for $\alpha = -1$, $R = 0.1$, $y_c = 0$ and $\ell = 0$ for various values of U. (**a**) $U = 0$, (**b**) $U = 1$, (**c**) $U = 2$, (**d**) $U = 3$, (**e**) $U = 4$, (**f**) $U = 5$. The values of ψ range from -10 to 10 in increments of 0.2

lubrication solution, and Sharatchandra et al. [3] who perform a complete Navier–Stokes simulation. For zero torque Day and Stone [5] and Matthews and Hill [6] demonstrate that for a cylinder placed closer to the bottom wall that the rotation direction is clockwise, which in this analysis implies $\alpha < 0$ and $y_c > 0$ and this agrees well with Eq. 4.9. Also, the lubrication solution shows that for a centrally placed rotating cylinder the torque is directly proportional to the rotation rate. Here a centrally placed rotating cylinder corresponds to $y_c = 0$, and Eq. 4.9 shows that in this case the same is true. Concerning the complete Navier–Stokes simulations performed by Sharatchandra et al. [3], their computed streamlines show that for a clockwise-rotating cylinder placed below the midpoint between the upper and lower walls (that is, below the location of the maximum external velocity), two symmetric co-rotating vortices exist above the cylinder, which is consistent with the experimental results of Sen et al. [1]. For small offsets the vortices are "squeezed" downwards on either side of the cylinder, while as the offset is increased, the two vortices

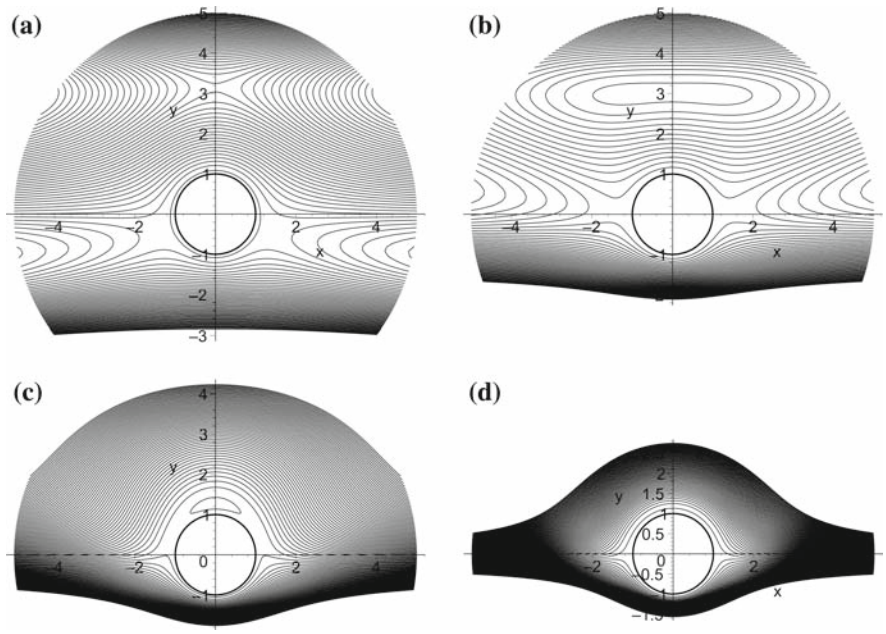

Fig. 3 Streamline plots for $\alpha = -1$, $R = 0.1$, $U = 3$ and $\ell = 0$ for various values of y_c. (**a**) $y_c = 1$, (**b**) $y_c = 2$, (**c**) $y_c = 3$, (**d**) $y_c = 4$. The values of ψ range from -10 to 10 in increments of 0.2

move above the cylinder and merge, initially as an outer vortex surrounding two inner co-rotating vortices, then as one large vortex directly above the cylinder. Our asymptotic analysis does not predict the existence of two separate vortices, since the effects of the upper and lower walls are not taken into account here. However, it can be envisaged that where the streamlines are reversed above the cylinder, as shown in Figs. 2d and 3a, in the presence of an upper wall these areas would be closer to the cylinder and may even close to form eddies. As y_c is increased, Figs. 3b and 3c show the existence of one single vortex directly above the cylinder. This is in partial agreement with [1], but as already noted that by increasing y_c further, the solution becomes like that for uniform flow, as shown in Fig. 3d.

Finally, we turn our attention to the effects of slip. Figures 2d and 4 illustrate streamline plots for $\alpha = -1$, $R = 0.1$, $U = 3$ and $y_c = 0$ for various values of ℓ. It can be seen that the streamlines for $\ell > 0$ are closer to the cylinder than for $\ell = 0$, in agreement with the findings of Matthews and Hill [10] for the case of uniform flow past a cylinder. It is interesting to identify the effect of slip on the behavior of the flow below the cylinder. For $\ell = 0$ it can be seen from Fig. 2d that the symmetry on the two sides of the x-axis is destroyed while the cylinder rotates, but from Fig. 4 we see that as ℓ increases from zero, the loss of symmetry is far less severe for the same values of the stream function. The reason for this behavior is as follows. The amount of slip is positive in the direction of the parabolic flow (from left to right) and the cylinder is rotating in a clockwise direction, hence on the lower half of the cylinder there is a balance between the rotation flow dragging the fluid from right to left, which is opposite to the slip effect which tends to allow the fluid to flow more easily from left to right. This balance between these absolute velocities results in the fluid being sheared less in this area, resulting in the smoother flow patterns. This would imply that the flow pattern below the cylinder behaves like the case of uniform flow past a non-rotating cylinder. This observation could be important for the design and implementation of devices such as the viscous pump.

Figures 3b and 5 illustrate streamline plots for $\alpha = -1$, $R = 0.1$, $U = 3$ and $y_c = 2$ for various values of ℓ. For this case the effects of slip are not as noticeable as for the case $y_c = 0$. The streamlines are closer to the cylinder than for $\ell = 0$, particularly the reversed streamlines to the left and the right of the cylinder. However, the vortex above the cylinder increases very slightly, but essentially remains unchanged in the presence of slip.

Equation 4.5 shows an expression for the frictional drag, and comparing this result with that for uniform slip flow past a cylinder presented in [10], we see that these results contradict each other, in the sense that Matthews and

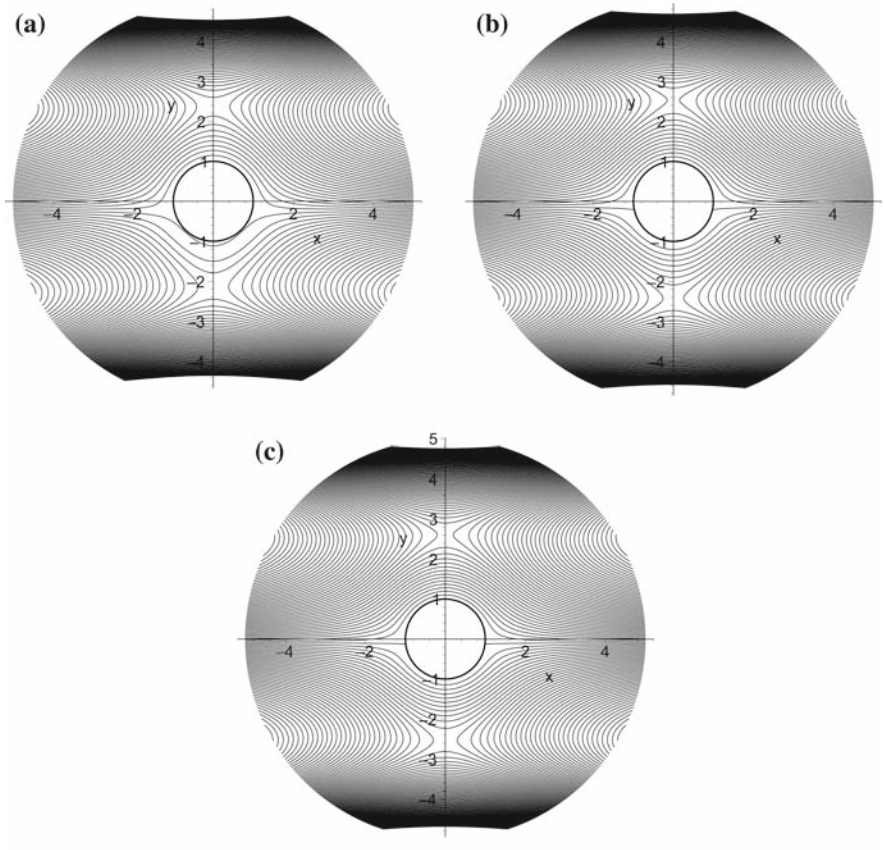

Fig. 4 Streamline plots for $\alpha = -1$, $R = 0.1$, $U = 3$ and $y_c = 0$ for various values of ℓ. (**a**) $\ell = 0.2$, (**b**) $\ell = 0.6$, (**c**) $\ell = 1.0$. The values of ψ range from -10 to 10 in increments of 0.2

Hill [10] observe that the frictional drag for $\ell > 0$ is reduced below the values for $\ell = 0$, whereas here we find the opposite. The reason for this discrepancy is due to the fact that we are using an altered definition of the Reynolds number than that of [10], and we have only carried out the analysis to first order. Higher-order corrections would change this conclusion, because in the limit of large U the results presented here reduce to those for leading-order uniform flow past a cylinder. Note that the leading-order expression for the frictional drag for uniform flow past a cylinder is given by

$$c_D = \frac{4\pi f_0(R)}{R}, \tag{5.1}$$

where

$$f_0(R) = \left[\log\left(\frac{1}{R}\right)\right]^{-1}, \tag{5.2}$$

which is independent of the slip length ℓ. The expression for the torque, given by Eq. 4.9, shows a very different effect of the slip length. By increasing the slip length we see that the torque is reduced. We can view this another way: for nonzero values of ℓ and a fixed value of the torque L, the magnitude of the rotation rate is increased. This agrees well with the findings of Matthews and Hill [6], where the lubrication solution demonstrates that the performance of the viscous pump is greatly improved by the inclusion of slip. This, of course, is to be expected since the reason the viscous pump works is because it operates at a scale where slip effects are important.

In this study we have attempted to ascertain the effects of slip on the performance of the viscous micro/nano pump by utilizing an approximate analytical solution, and further experimental and numerical studies are required

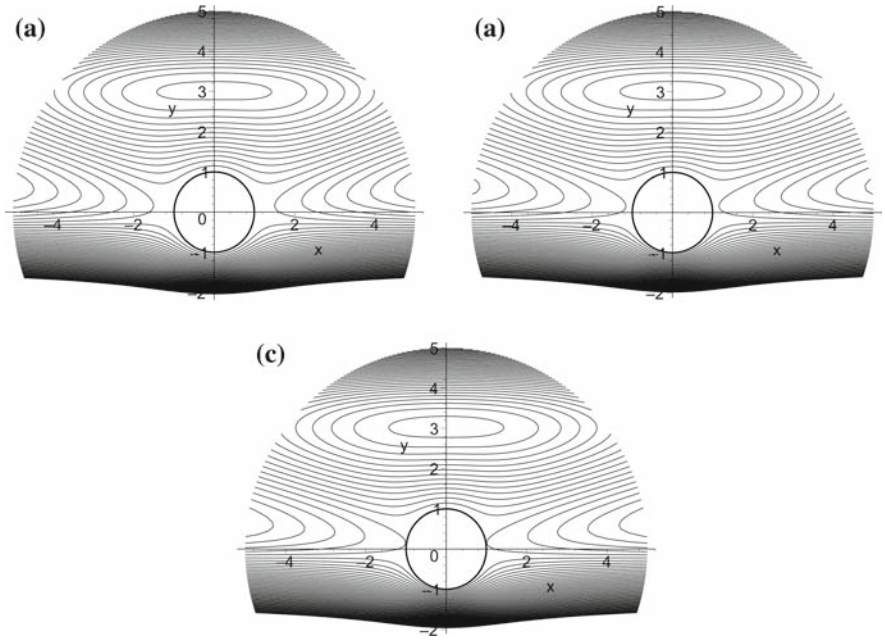

Fig. 5 Streamline plots for $\alpha = -1$, $R = 0.1$, $U = 3$ and $y_c = 2$ for various values of ℓ. (**a**) $\ell = 0.2$, (**b**) $\ell = 0.6$, (**c**) $\ell = 1.0$. The values of ψ range from -10 to 10 in increments of 0.2

to validate our slip solutions. In particular, the construction and experimental study of a viscous pump comprising hydrophobic or hydrophilic materials, which would promote the slip effects studied here, would possibly demonstrate the vastly improved performance of such a device.

Acknowledgements This work is funded by the Discovery Project scheme of the Australian Research Council, and the authors gratefully acknowledge this support. JMH is grateful to the Australian Research Council for provision of an Australian Professorial Fellowship.

References

1. Sen M, Wajerski D, Gad-el-Hak M (1996) A novel pump for MEMS applications. J Fluids Eng 118:624–627
2. Abdelgawad M, Hassan I, Esmail N (2004) Transient behavior of the viscous micropump. Microscale Thermophys Eng J 8:361–381
3. Sharatchandra MC, Sen M, Gad-el-Hak M (1997) Navier–Stokes simulation of a novel viscous pump. J Fluids Eng 119:372–382
4. Sharatchandra MC, Sen M, Gad-el-Hak M (1998) Thermal aspects of a novel viscous pump. J Heat Trans 120:99–107
5. Day RF, Stone HA (2000) Lubrication analysis and boundary integral simulations of a viscous micropump. J Fluid Mech 416:197–216
6. Matthews MT, Hill JM (2006) Lubrication analysis of the viscous micro/nano pump with slip. Microfluid Nanofluid 4:439–449
7. Stokes GG (1851) On the effect of the internal friction of fluids on the motion of pendulums. Trans Cambr Philos Soc 9:8–106
8. Proudman I, Pearson JRA (1957) Expansions at small Reynolds number for the flow past a sphere and circular cylinder. J Fluid Mech 2:237–262
9. Van Dyke M (1975) Perturbation methods in fluid mechanics. The Parabolic Press, Stanford
10. Matthews MT, Hill JM (2006) Flow around nanospheres and nanocylinders. Quart J Mech Appl Math 59:191–210
11. Bretherton FP (1962) Slow viscous motion round a cylinder in a simple shear. J Fluid Mech 12:591–613
12. Robertson CR, Acrivos A (1975) Low Reynolds number shear flow past a rotating circular cylinder. Part 1. Momentum transfer. J Fluid Mech 40:685–704
13. Majhi SN, Vasudevaiah M (1982) Flow separation in a viscous parabolic shear past a sphere. Acta Mechanica 45:233–249
14. Nguyen NT, Wereley ST (2006) Fundamentals and applications of microfluidics. Artech House, Norwood
15. Karniadakis G, Beskok A, Aluru N (2005) Microflows and nanoflows fundamentals and simulation. Springer, New York

16. Navier CLMH (1823) Mémoire sur les lois du mouvement des fluides. Mémoires de l'Académie Royale des Sciences de l'Institut de France 6:389–440
17. Matthews MT, Hill JM (2006) Micro/nano sliding plate problem with Navier boundary condition. Zeitschrift für Angewandte Mathematik und Physik (ZAMP) 57:875–903
18. Happel J, Brenner H (1965) Low Reynolds number hydrodynamics. Prentice-Hall, New Jersey
19. Slattery JC (1999) Advanced transport phenomena. Cambridge University Press, Cambridge
20. Robertson CR (1969) Ph.D. thesis, Stanford University
21. Kaplun S (1957) Low Reynolds number flow past a circular cylinder. J Math Mech 6:595–603